A new cold cooling system using krypton for the future upgrade of the LHC after the Long Shutdown 4 (LS4)

Luca Contiero[a,b,1], Bart Verlaat[a], Armin Hafner[b], Krzysztof Banasiak[c] , Yosr Allouche [b], Paolo Petagna[a]

[a] European Organization for Nuclear Research, Geneva, 1211, Switzerland,
[b] Norwegian University of Science and Technology, Trondheim, 7491, Norway
[c] SINTEF Energi AS, Trondheim, 7034, Norway

ABSTRACT

Future silicon detectors for High Energy Physics Experiments will require operation at lower temperatures to cope with radiation damage of the sensors and consequent increase of the dark current, beyond the limit of the current CO_2 evaporative cooling system. This, together with many other requirements such as mass minimization and high radiation hardness, pushes the need of a new advanced cooling technology. The new coolant shall be able to approach ultra-low temperatures below -60 °C, withstand high radiation levels while having cooling lines diameters comparable to the currently achieved with the CO_2 technology. Among different natural working fluids, krypton appears as a promising coolant for the thermal management of future detectors in high-irradiated environments. The thermodynamic properties of krypton do not allow the use of a pumped loop cycle but rather impose a need of a novel cooling technology. A new ejector-supported krypton cycle is presented, highlighting the cycle dynamics involved due to the different temperature levels normally encountered during the detector lifetime.

Keywords: Krypton, CO_2, Detector, Supercritical, Ejector, Cooling

1. Introduction

Silicon detector trackers are used in High-Energy Physics (HEP) experiments to track the path and momentum of particles created by the collisions inside the beam pipe. Those sensors are uniformly distributed along the detector volume. Construction material used around the detector must be tolerant of ionizing radiation and of low mass density. The wanted signals from charged particles crossing those sensors are very short pulses of current. The dark current of the sensors has to be kept low by low operating temperatures and the heat generated by the dark current in the sensor and the heat of surrounding electronics needs to be removed by the cooling system to maintain the sensors thermally stable after radiation damage, preventing the phenomena of thermal runaway [1]. Different generation of detectors have required over the years a continuous upgrade of the cooling system according to the thermal requirements. In the 1990s, single phase cooling with water under sub-atmospheric pressures was used but drawbacks such as water freezing point and low efficiency in

[1] Corresponding author at: European Organization for Nuclear Research, Geneva 1211, Switzerland.
E-mail addresses: luca.contiero@cern.ch / luca.contiero@ntnu.no (L. Contiero), bart.verlaat@cern.ch (B. Verlaat), armin.hafner@ntnu.no (A. Hafner), krzysztof.banasiak@sintef.no (K. Banasiak), yosr.allouche@ntnu.no (Y. Allouche), paolo.petagna@cern.ch (P. Petagna).

terms of heat removal capability of the fluid made two-phase cooling the preferred choice [2]. Alternatively, mixture of water and glycol was also considered.

One advantage of evaporative cooling is the isothermal extraction of the heat (the two-phase fluid temperature does not change other than due to pressure drops along the cooling pipe).In the ATLAS ID an evaporative cooling system based on perfluorocarbons C_3F_8 [3] is used, which provides low evaporation temperature with a low pressure fluid, while presenting a high radiation hardness. Low-operating pressure allows for thinner tube wall, reducing the mass but as drawback the tube size is increased to limit the pressure drops and related temperature drops which are amplified by the low reduced pressure. The system was firstly based on a compression driven cycle before being changed to a gravity-driven thermosyphon cycle [4]. The latter has the advantage that it avoids the challenges deriving from employment of oil-free compression, which normally requires much more maintenance than oil-lubricated machines. In contrast, single-phase cooling using C_6F_{14} was used for the CMS detector tracker via a pumped loop cycle since it was considered more robust than relying on a large two-phase system for which there existed little experience at the time. Despite the high-radiation hardness of C_3F_8, CO_2 has proven to have excellent thermal performance in small-diameter-tube evaporators which is extremely welcome for low-mass detector design [5]. A mechanically pumped loop concept with a two-phase accumulator was developed at NIKHEF [6] for the Alpha Magnetic Spectrometer (AMS) for the International Space Station (ISS) and used in the Vertex Locator (Velo) of the LHCb detector [7]. The suitability of CO_2 to withstand high radiation with excellent thermophysical properties, as well as ensuring a remote control of the detector operational temperature, have led to the adoption of CO2 evaporative cooling systems in other detectors at CERN, CMS Pixel detector [8] and the ATLAS IBL tracking layer [9]. However, the freezing point of CO_2 and the subcooling required at the pump inlet limit the use of the 2PACL for the ultra-low temperature range [10].

Since CO_2 cannot be used at these very low evaporation temperatures, a new environmental and performant coolant must be identified [11,12]. In this article different natural working fluids are compared, considering relevant thermophysical properties and their thermal performance. Among different candidates, krypton is a promising candidate and its thermophysical properties have been studied to design and propose a suitable cooling technology. The new cooling concept developed allows to provide cooling either in supercritical cold conditions or under flow boiling at the detector. Even though the control strategy presented is designed primarily for detector cooling, the working principle can be extended to any other cooling system operating in the supercritical area which requires a slow and controlled cooling in case the object to be cooled is sensitive to fast temperature gradients that could potentially harm its integrity.

2. Challenges for cooling of silicon detectors in High Energy Physics

Detector cooling presents peculiarities that go beyond any conventional refrigeration system in terms of available space, reliability, maintenance, amount of heat dissipated and maximum ΔT allowed between inlet-outlet. The hardware for cooling inside the detector must be minimized through efficient system-level solution. In this respect, the use of a working fluid enabling the integration of small cooling channels while concurrently preserving high thermal performance throughout the pipe, is of primary importance. The trackers require long cooling lines to reach all the heat sources. Refrigerants should have low global warming potential and be radiation hard. It is known that traditional fluids containing hydrogen in their molecular composition could decompose due to the phenomena of molecular chain breaking [13]. A range of working fluids, comprising nitrous oxide, ethane and ethylene, and the noble gases krypton and xenon, has been compared for the ultra-low temperature range. Potential interesting mixtures as CO_2+N_2O have not been considered since their thermal performance will not differ substantially from that of pure fluids.

Nitrous oxide has similar properties to CO_2 but a lower freezing point, making it suitable to be used as a freezing depressant [14]. However, the operating pressure remains extremely low leading to poor thermal performance due to the high dependency of temperature on the vapor pressure at low reduced pressure, which in turns would negatively affect the temperature of the sensors according to the heat path of the fluid. Furthermore, N_2O is an oxidizing agent which can decompose explosively under specific conditions and therefore its use in pure form is not recommended [15]. A mixture of CO_2 and N_2O can alleviate this issue but on the other hand the minimum possible operating temperature constrained by the freezing point rises as a function of the CO_2 concentration in the mixture. The hydrocarbons ethane and ethylene present interesting thermal properties but they are flammable, limiting their use due to safety concerns. In addition, if a further extension of the operating envelope towards colder temperatures is required, these coolants have in the normal boiling point (NBP) their limitation (-88.58°C for ethane and -103.8°C for ethylene). Operating below the NBP would require working under vacuum conditions and increases the risk of air infiltration into the system causing performance degradation. In case of an air infiltration into the system, the presence of non-condensable gases (i.e. nitrogen) can partially clog capillary tubes, creating intermittent unbalance of the mass flow rates along the cycle and increasing the power consumption of the system due to sudden reduction of the cooling capacity. If this happens, the system needs to be stopped and the entire refrigerant charge recovered before proceeding with the new filling. This points out the importance of the NBP as limiting factor in the fluid selection. The noble gases xenon and especially krypton have low NBP and they are the most stable elements in nature, which is certainly an attractive quality [16]. It is worth to mention that CO_2 is a fluid with unique physical properties: the other fluids previously mentioned have a freezing point at very low pressures, significantly below the atmospheric pressure. Nonetheless, when considering thermal performance, it is crucial to focus on the NBP of these fluids. The thermal performance comparison of different fluids will be based on relevant thermophysical properties such as latent heat of vaporization, viscosity, surface tension and liquid-vapor density ratio (Figure 1).

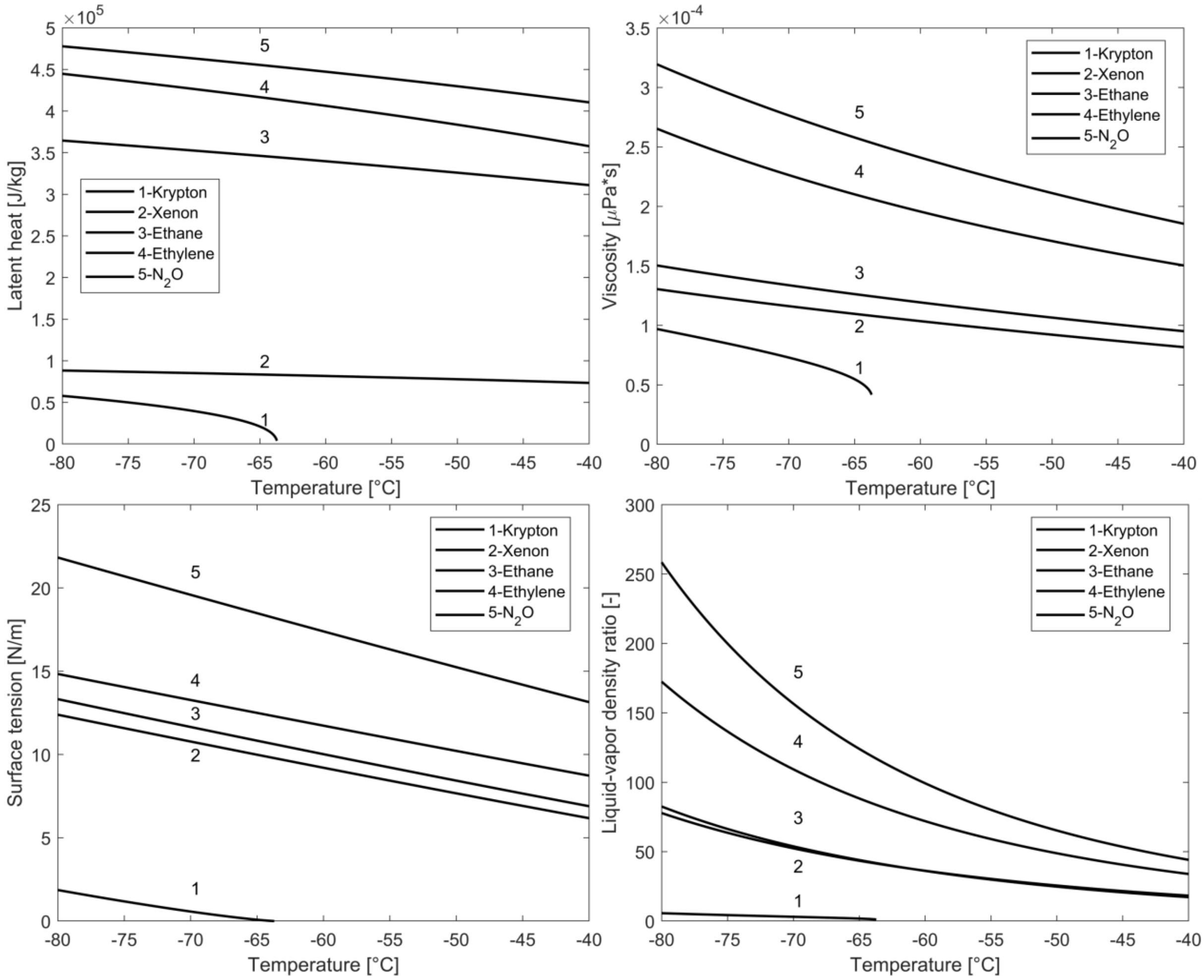

Figure 1: Relevant thermodynamic properties of the fluids investigated.

Latent heat represents the total amount of heat that is absorbed by a fluid before completely turning into vapor. A larger latent heat is normally preferred since the flow can be reduced and consequently the associated pressure gradients are smaller. The dynamic viscosity is a measure of the resistance of a fluid to flow, while surface tension indicates the forces holding the molecules together that must be overcome to initiate the boiling process. The ratio of liquid to vapor density is more complex: in two-phase flow a low-density ratio promotes a more homogenous flow, impacting flow pattern and heat transfer. More importantly, a high-density ratio causes larger pressure drops between inlet and outlet, causing an uneven temperature distribution. Therefore, having a fluid with high vapor density results in lower temperature drops for the same pressure drops.

In the range between -60 to -80 °C [12], it is important to distinguish between the two-phase and supercritical state of krypton which has a critical temperature around -64 °C. Above this temperature, sharp changes in fluid density as well as in the heat capacity occur. Two-phase cooling at high pressures presents extremely high heat transfer coefficients and small volume thanks to gas compression whilst supercritical fluids near the critical point present smaller values of heat transfer [17] but low pressure drops thanks to low viscosity levels. However, the advantages of two-phase cooling are strongly dependent on operating pressure and molecular weight of the fluid. Supercritical fluids are especially interesting because of the high heat capacity and low resistance to flow in proximity of the pseudocritical points. A pseudocritical point is the thermodynamic condition given by a temperature and pressure above the critical values at which a maximum of specific heat capacity is registered. Peaks in specific heat capacity and thermal conductivity quickly decrease as we move away from the critical point. The temperature distribution of a fluid can be understood through its specific heat capacity. When the specific heat capacity is larger, the behavior of a supercritical fluid resembles that of a two-phase fluid thanks to a nearly constant temperature profile. For cooling of detector trackers where heat transfer performances are crucial for the thermal management of the sensors, working in proximity of those pseudocritical points seems beneficial.

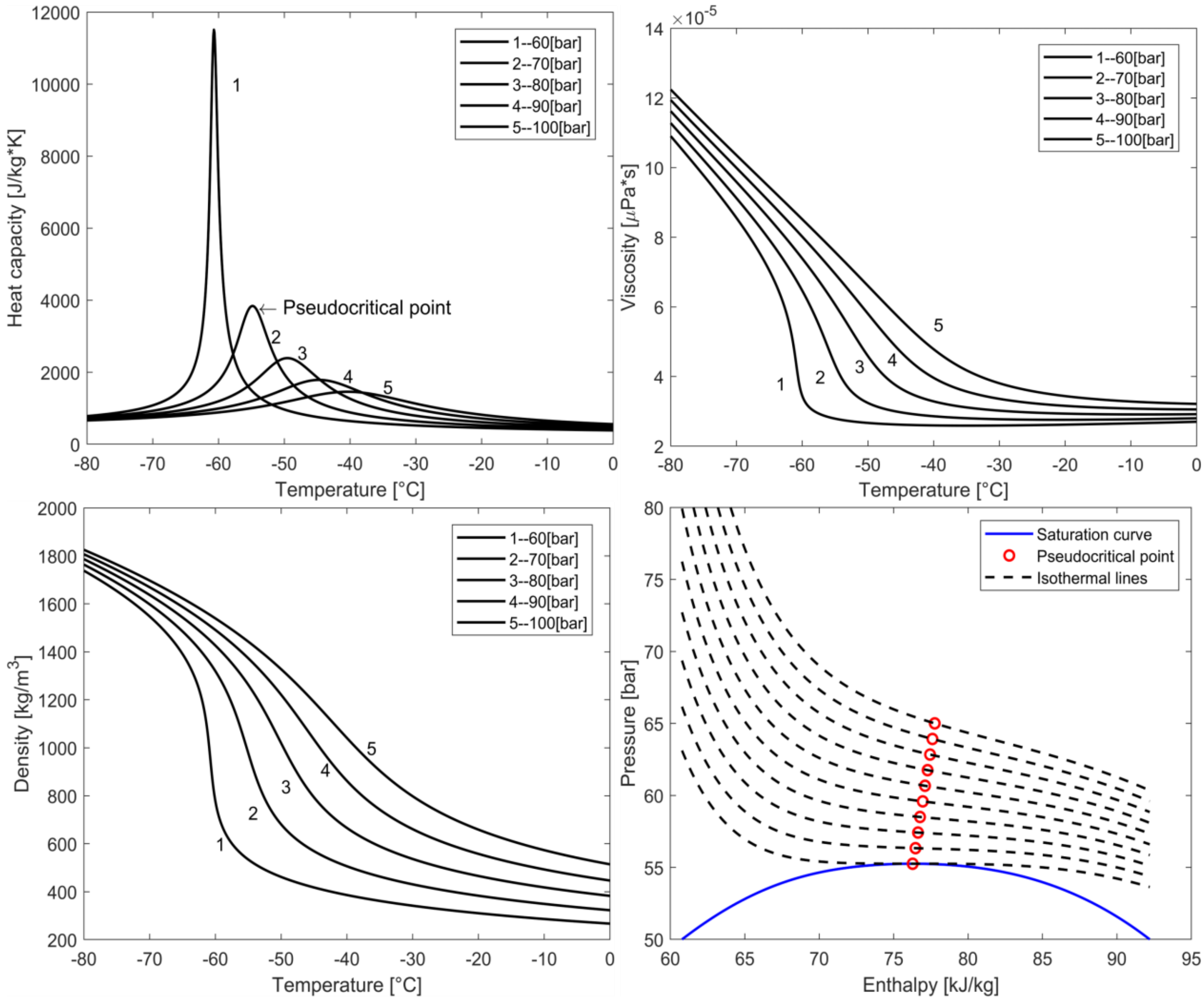

Figure 2: Thermodynamic properties of supercritical krypton at different pressures and temperatures.

This mono-phase region is not only interesting in mini-channel applications but also for micro-channels. In two-phase systems using micro-channels, fluid resistance given by micro-orifices are required at the channel inlet to promote an even flow distribution and suppress flow instabilities. This challenge is of a great importance to avoid risk of dry-out considering that micro-channels are much more susceptible to flow maldistribution than mini-channels. Two-phase flow in micro-channels imperatively requires collecting the flow exiting each channel in the outlet manifold: the hindrance posed by the two-phase state of the flow for further flow distribution in the subsequent channel becomes feasible by employing a supercritical fluid. In supercritical state, all the flow can pass by multiple chips in series rather than being distributed through multiple channels in parallel [18] as would occur in a two-phase distribution system. The thermal budget in terms of ΔT-ΔP would pose the number of how many chips can be efficiently cooled by one single stream. Although supercritical fluids could offer a remarkable alternative to two-phase cooling while preserving the advantages of single-phase fluids, their characterization is still far from the well-known two-phase area. For this reason, the natural working fluids studied here are all compared under boiling conditions.

3. Fluid study comparison

Although the optimization of the cooling system comprises the fluid but also the support of the cooling structure in which the fluid is embedded, a single fluid-based approach has been used here [13]. The optimal physical performance of the detector requires the mass minimization of the full structure around it. Mass minimization normally refers to a parameter called radiation length [19] which is a scale of length for the degradation of particle trajectories due to scattering and radiation. In principle this means that a smaller cooling tube does not necessarily lead to the best scenario if the missing volume is replaced by a material with a shorter radiation length. The simplest way to identify the most promising coolant in HEP is to use a non-conventional definition of the thermal performance of a fluid: the volumetric heat transfer coefficient as defined in Eq. (1).

$$\boldsymbol{VHTC} = \frac{\boldsymbol{Q}}{\boldsymbol{Volume} * (\boldsymbol{\Delta T}(\Delta \mathrm{p}) + \boldsymbol{\Delta T}(\boldsymbol{HTC}))} \quad (1)$$

Unlike the conventional definition of the heat transfer coefficient that measures locally the thermal performance of the fluid, the volumetric heat transfer coefficient is a scan of the overall performance of the fluid for a given operating condition and tube geometry. It combines important requirements for the detector that need to be fulfilled to achieve an efficient cooling:

- low temperature losses on the fluid side, as a function of the fluid pressure drops and therefore described via the term ΔT(Δp).
- Minimization of the Thermal Figure of Merit (TFM), a parameter normally used within the detector community to quantify the efficiency of the conductive (through tube wall and materials surrounding the cooling pipe) and convective (fluid dependent) heat transfer processes. High heat transfer coefficients make the applied cooling method more efficient, contributing to the minimization of convective term described in the VHTC as ΔT(HTC). The conductive term is a function of the thermal impedance of the passive resistance of the support structure.

The warmest point during flow boiling is normally located at the entrance of the pipe where the fluid temperature and pressure is highest. The tube diameter has an impact on longitudinal gradients in terms of pressure and temperature, which in turns affect the heat transfer coefficient and the temperature gradient along the heat path sensor-cooling tube (transversal gradient).

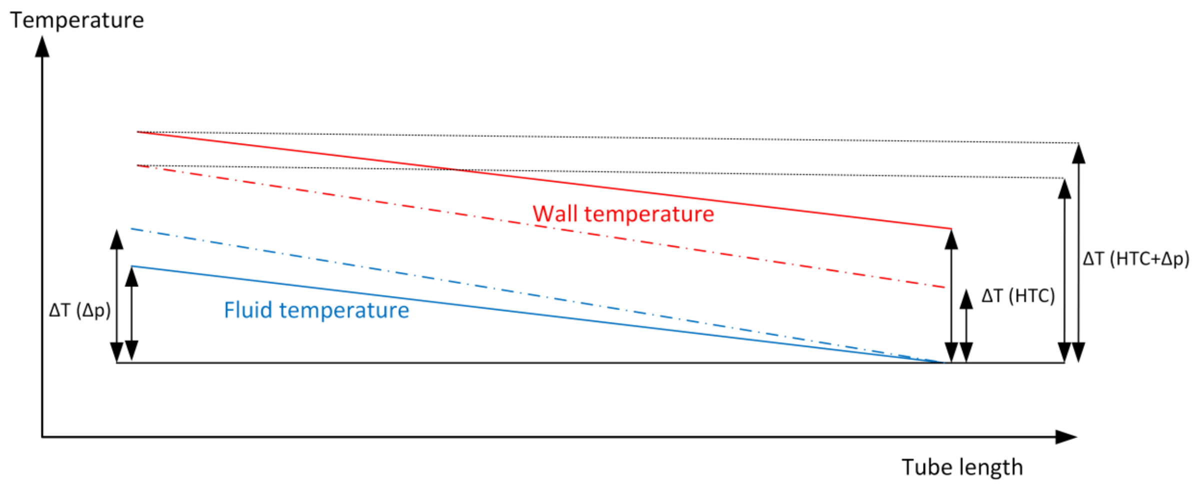

Figure 3: Typical temperature distribution along a two-phase cooling tube where temperature gradients with respect to pressure drops and local heat transfer coefficients are illustrated (dotted lines illustrate the case with reduced diameter).

The volumetric heat transfer has been calculated using MATLAB [20], where correlations of heat transfer (Kandlikar [21] and pressure drop (Friedel [22]) have been implemented. The outlet pressure and quality are fixed, therefore requiring an iterative solution to find the mass flow rate entering the detector under saturated conditions. Figure 4 gives a graphical representation of the volumetric heat transfer coefficient considering a typical detector cooling pipe: the optimum tube diameter can be calculated as a trade-off between an increase of the flow speed and larger pressure gradients.

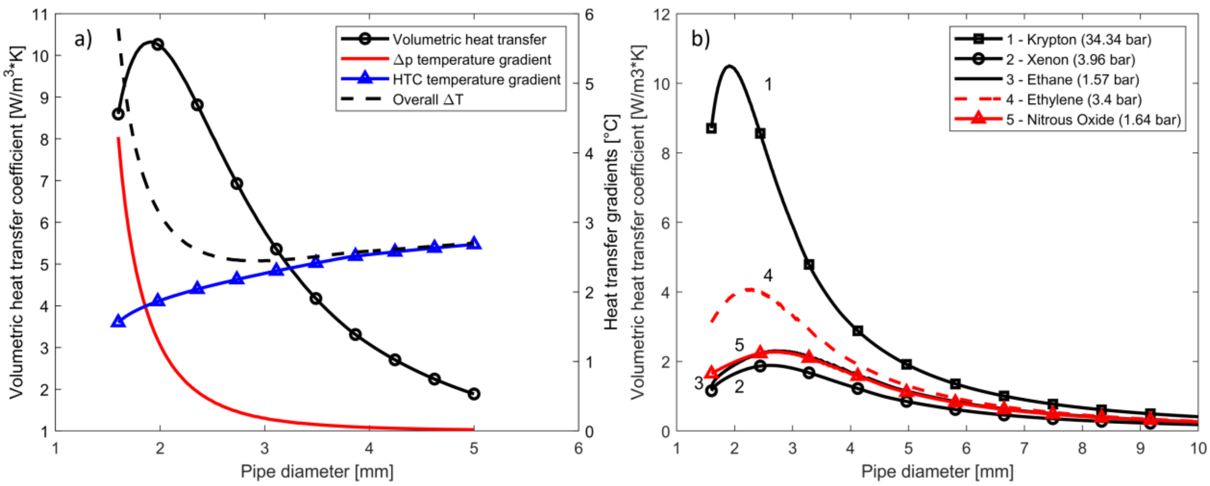

Figure 4: Cooling tube performance optimization for krypton (a) & comparison of the VHTC of the different fluids investigated (b) considering standard detector geometry (length = 2[m], Q = 200[W], outlet vapor quality = 35%, T = -80 °C]).

In the same manner, all the other fluids have been compared. The noble gas krypton outperforms the other candidates showing a peak in the volumetric heat transfer around a diameter of 2 mm, in the same order of what is currently used in the CO_2 cooling system [23]. The main reason is the operating pressure: at higher pressures the temperature drops are less sensitive to pressure drops, the vapor phase remains more compressed allowing a volume reduction of the pipe. Other potential candidates, especially N_2O and Xenon, are low-pressure fluids and thus extremely sensitive to pressure drops. Their optimal diameters are larger, and they have a lower heat transfer maximum. Figure 5 shows the estimated volumetric heat transfer coefficients for a wide range of temperatures, including the warmer range where CO_2 is identified as the most performant and neutral (not flammable and toxic) coolant. The perfluorocarbon C_3F_8 has much worse thermal performance compared to all the others, while being a banned fluid nowadays. It is worth to notice that the maximum performance is registered in proximity of the critical point where the specific heat capacity is maximum, despite the low latent heat which tends to zero at the critical point. For the ultra-low temperature range krypton stands out as the best candidate for thermal management of future detectors.

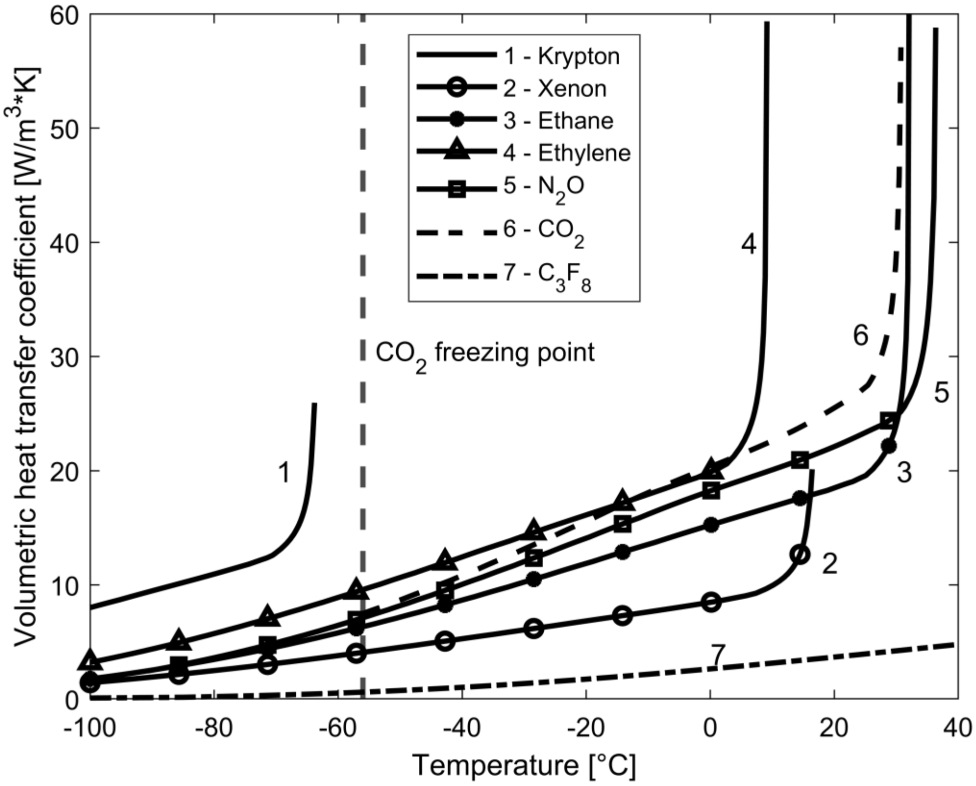

Figure 5: Comparison VHTC for different fluids over a wide range of temperatures.

4. Challenges with krypton cooling

As demonstrated above, the noble gas krypton outperforms all the other candidates in the temperature range of interest. Regardless of the associated cooling system, silicon detector trackers require during their lifetime to be kept at different temperature levels. For instance, during the commissioning phase, cooling around ambient conditions is needed. Therefore, the cooling system must be able to cool down the trackers under all intermediate temperature levels in a stable manner, while guaranteeing to remove the heat dissipated from the sensors that can vary from full load to no load according to the type of detector. Those constraints, together with the thermophysical properties of krypton, pose challenges never experienced before both with the old cooling system using C_3F_8 [3] and the current 2PACL [24] using CO_2. Indeed, those refrigerants at ambient conditions are in liquid phase, or vapor or two-phase state according to the charge of fluid in the system. Figure 6 represents the pressure-enthalpy diagram of krypton: at ambient conditions it is in gas/supercritical state according to the the amount of refrigerant charge in the system, where there is no distinction between phases (liquid-vapor).

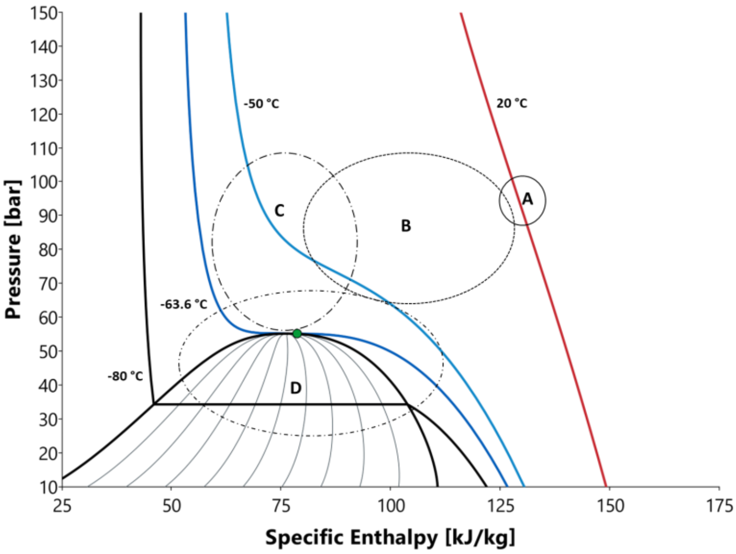

Figure 6: Pressure-enthalpy diagram of krypton, highlighting the most important isothermal lines and the different working regimes encountered during the detector lifetime. The zones A-D are explained in the text.

At room temperature (zone A), the fluid behaves as gas and it does not allow the use of a pumped loop cycle as currently in use for the CO_2 cooling. The use of a vapor compression system poses many challenges: firstly, the system must rely on oil-free machines such as turbocompressors, since it is very hard to avoid oil contamination in the refrigerant going through the detectors. If this happens, under strong irradiation the oil droplets could polymerize potentially clogging the cooling lines or produce corrosive compounds. Secondly, designing a turbomachine for a wide range of operating conditions is challenging, mainly due to density changes while moving from the warm to the cold state. At last, during the startup, the activation of the compressor may cause a thermal shock in the detector. Indeed, in any refrigeration system the compressor startup causes a rapid decrease of the suction pressure which is associated with a temperature drop. In a detector application this may lead to undesirable fluctuations of the fluid temperature entering the detector. As common practice in particle detectors, a gradual and controlled cooldown of about 1 K/min is desirable [13]. Figure 6 highlights all the transient scenarios encountered by the detector: start-up (A), supercritical cooldown (B), supercritical operation (C), transcritical operation (D) including the transition mode between supercritical to two-phase mode. Different working envelopes involve different control strategies (always prioritizing the detectors), due to the significant distinction between the supercritical and two-phase states. In the supercritical zone, the fluid behaves as a single-phase fluid, whereas in the two-phase state, there is a coexistence of liquid and vapor phase. As a result, the regulation of pressure is carried out in completely different manners. The amount of refrigerant stored in the cycle determines the achievable pressure levels. It is common practice in any vapor compression system to have a separator to help deliver only vapor to the compressor suction port while liquid to the evaporator section. In the two-phase state, the liquid separator functions as a buffer tank, and it is used to manage refrigerant charge fluctuations due to variation in system pressures, unsteady operation caused by sudden changes in the evaporator load (i.e. detector heat load) and variability of external conditions. Conversely, in the supercritical state, adjusting the pressure to the desired level can only be achieved through the injection or removal of refrigerant charge from the cycle. In addition, in supercritical state pressure and temperature are independent of each other and therefore pressure control does not necessarily impose control of temperature.

5. Ejector as flow regulator through the detector

The evaporative cooling system using C_3F_8 had a similar functionality to that of a standard vapor compression cycle. Because of the already explained requirements and preferred working area involving low-vapor quality regimes, heaters were placed inside the detector to allow for warm return lines, thus eliminating the need of thermal insulation as well as the risk of compressor damage in presence of liquid droplets. From an energy point of view, electrical heating is an inefficient way that can be overcome by means of an ejector. In a traditional vapor-compression cycle isenthalpic expansion is an irreversible process that constantly generates entropy while expanding. For some fluids exergetic losses are quite remarkable and they limit the coefficient of performance of the system, as occurring in CO_2 systems during transcritical operation [25,26]. A simple and cost-efficient way of using the potential energy of the expanding fluid is an ejector [27], being a robust component that involves no moving parts (Figure 7).

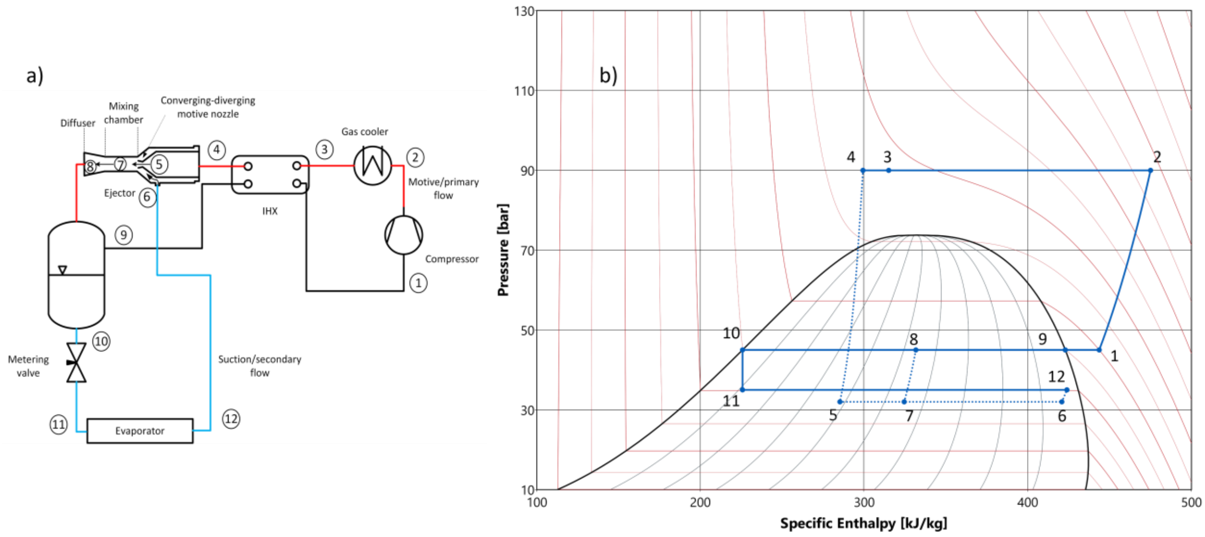

Figure 7: System layout of transcritical ejector CO_2 system (a) & representation in the p-h diagram (b).

The fluid exiting the high-pressure gas cooler section (point 4) is normally called primary or motive flow, while the entrained flow from the evaporator outlet (point 12) is called secondary or suction flow. The primary flow is expanded through a nozzle, accelerating up to sonic conditions (Mach n° = 1) and further accelerates to supersonic conditions in the nozzle diverging section (point 5). The increase of kinetic energy corresponds to a pressure decrease which by means of a local depressurization zone (point 5) drives the flow from the secondary inlet (point 12) into the suction chamber (point 6). The two streams are then mixed in the mixing chamber (point 7) where they exchange mass, momentum and heat. The flow is later decelerating in the diffuser where there is an increase of static pressure, which corresponds to the diverging area located at the ejector outlet. Normally two parameters are computed to describe the ejector performance: mass entrainment ratio and pressure lift (Eq. (2)-((**3**), respectively where the subscripts indicate the thermodynamic state referred to Figure 7).

$$\boldsymbol{\Theta_m = \frac{\dot{m}_{12}}{\dot{m}_4}} \quad (2)$$

$$\boldsymbol{P_{lift} = p_8 - p_7} \quad (3)$$

Those two parameters must be considered simultaneously because they measure two separate effects of the ejector. A given amount of kinetic energy in the motive flow can either be used to pre-compress a large amount of secondary flow across a small pressure difference or vice versa. A trade-off exists among those two quantities. However, attention should be given to the controllability of such device: if the ejector is static, i.e., with constant-geometry motive nozzle, the high-pressure side cannot be actively controlled, compromising the amount of the secondary flow entrained in part load. As consequence, the ejector will perform in a suboptimal way.

In a properly designed ejector, the convergent-divergent motive nozzle produces subsonic flow in the convergent section, reaching locally sonic condition at the throat (minimum cross-sectional area) and further accelerates to supersonic condition in the divergent area. The velocity will increase after the narrowest point from sonic to supersonic (Mach n° > 1) as the flow expands in the diverging section. The isentropic expansion of the primary flow to supersonic Mach number causes the static pressure and temperature to decrease from the throat to the pre-mixing chamber, hence the amount of expansion work defines the exit pressure and temperature. With a fixed geometry ejector it is not possible to adjust the mass flow rate while maintaining constant motive conditions in terms of temperature and pressure. When the motive flow reaches critical conditions, the secondary flow cannot be adjusted by manipulating the downstream pressures (discharge or suction pressures). The potential to entrain the secondary stream is strongly influenced by the high-pressure control which could result in no suction flow delivered during part-load operation in case of a static ejector. The secondary flow, which in this application refers to the krypton flow through the detector, owing to the entrainment effect can be adjusted in a controlled-geometry ejector using a needle that moves towards and away from the nozzle throat, regulating the flow by restricting or increasing the flow area [28,29].

6. Cold krypton cycle

The cycle presented here is an ejector-supported krypton cycle where the heat is rejected to a CO_2 system with the feature of controlling the evaporating level such to avoid excessive high temperature differences between the two fluids. It consists of a cascade refrigeration system where the high-temperature circuit is a primary transcritical CO_2 cooling unit, while the low-temperature circuit is the krypton unit connected to the detectors. It can maintain the refrigerant entering the detector area either in supercritical cold conditions or in subcritical conditions in subcooled state to ensure that in this latter case boiling starts at the entrance of the evaporator. Important features of the cycle are firstly the possibility to extend the temperature range towards colder temperature without a full upgrade of the cycle, and secondly the design of the cycle is based on the well-known two-phase area where expertise in the community exist, while the supercritical area has been less explored so far [12]. The simplified piping and instrumentation diagram (P&ID) of the cycle is illustrated below in Figure 8. The transition between different operating modes (supercritical – transcritical) is achieved by activating different components of the system in response to changes in the temperature and pressure level.

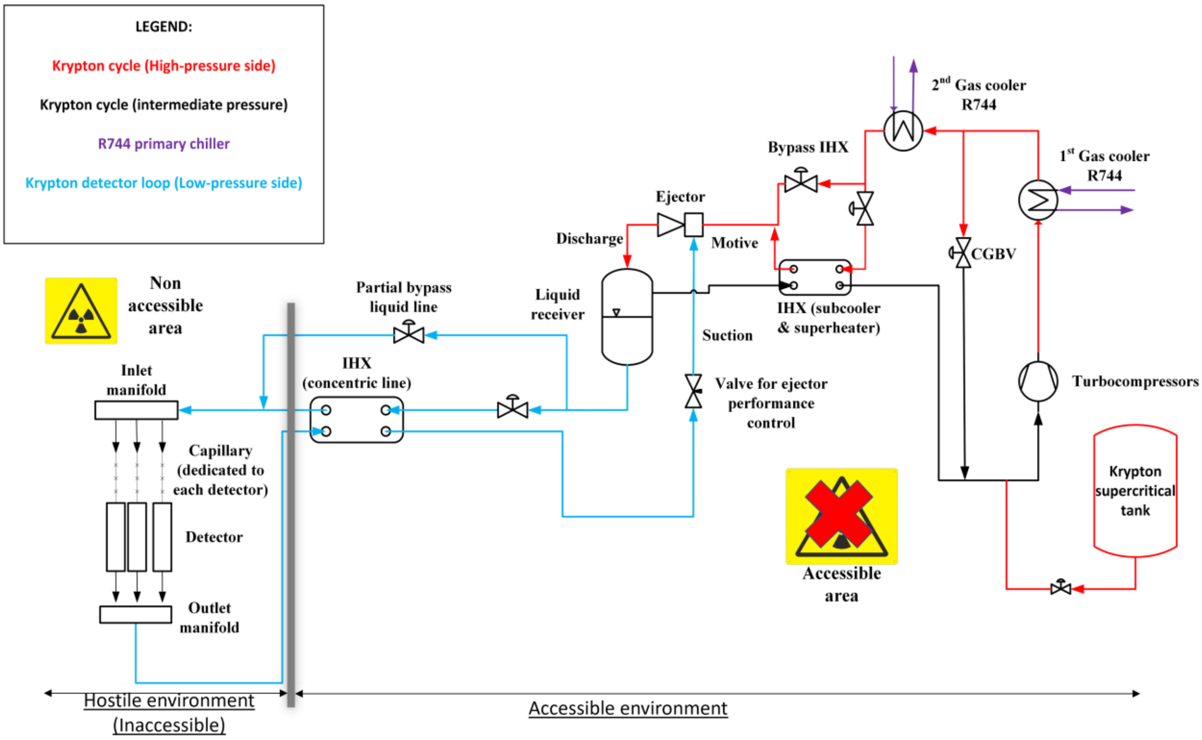

Figure 8: Simplified piping and instrumentation diagram (P&ID) of the krypton cooling unit.

The proposed ejector-supported cycle involves three different pressure levels: low (detector), intermediate and high-pressure level. The system comprises a compression stage, a gas cooler section with a bypass, an internal heat exchanger, a controllable-ejector geometry and a loop used to distribute the coolant to the detectors. The bypass (CGBV) downstream the first gas cooler serves as a flow regulator in opposition of a variable speed drive compressor, and it is chosen and used here to enhance the reliability and stability. A high-pressure tank is also used to condition the system prior to startup and to sustain supercritical operation during the gradual cooldown, by further injecting krypton into the system. The ejector works as a high-pressure control device while it enables recirculation of the cold fluid coming from the detector outlet by using the expansion work available, in a very similar manner to a traditional ejector vapor compression cycle [27]. The low-pressure side is very similar to what is in use nowadays with CO_2 within the 2PACL system: the long distance is covered by a tube-in-tube arrangement to shield the liquid from ambient heating, as well as due to space constraints. This counter-flow heat exchanger is needed for conditioning the evaporator inlet flow to a low vapor quality during flow boiling operation. Expansion devices such as capillaries are installed at the detector inlet to ensure expansion before starting boiling whilst promoting a homogenous distribution of the flow through the multiple parallel channels, considering that the heat loads in the individual branches can be different, and vary over time. Passive expansion devices must be used to the inaccessibility for maintenance in an irradiated environment. Because reliability is one of the main concerns, an expansion device is also installed immediately upstream the ejector suction nozzle: changing the opening of the valve allows to reduce the flow invoked by the ejector, substantially wasting part of the expansion work available in favor of one extra degree of freedom to control flow through the detector.

It should be noted that the ejector can potentially lift a large or small amount of flow according to the jump in pressure of the low-pressure fluid. In any conventional refrigeration system, trade-off among those quantities is controlled via a metering valve (Figure 7, point 10-11). In a detector application, passive expansion devices do not allow a regulation of the flow area but rather the pressure drop will increase quadratically as the flow increases. This emphasizes the need for a controllable ejector geometry as described in the Figure 9 below, which is developed considering a fixed outlet detector temperature (-70 °C). The graphical representation of the ejector and detector performance curves serves only as illustrative example, since the mass flow for a given pressure drop across the detector can be computed only for a specific geometry of the passive loop. The blue solid curve represents a typical ejector characteristic curve which remains unchanged under constant boundary conditions at the motive and suction nozzle. The entrainment ratio remains initially constant before dropping: this phenomenon is related todouble choked conditions in both motive and suction nozzles. The flow results to be choked when the fluid velocity reaches the speed of sound (sonic conditions) at the throat location and a further increase of the pressure difference does not lead to any increase of the mass flow rate. However, this curve will mainly vary according to changes in the motive rather than due to the suction conditions. The red curve represents the passive loop behavior as a function of the flow crossing the detector, normalized with respect to the motive flow to scale up the curve and have a fair comparison. For a specific operating temperature in the detector, one working point (flow) allows to remove the heat dissipated while guaranteeing an exhaust two-phase flow from the detector with a vapor content around 35% (indicated by the blue circle). Higher flows than the desired one would produce an overflow with a drastic increase of the liquid content at the detector outlet while a reduced flow leads to unstable scenario and possible dry-out (black filled area). The intersection of the detector and ejector curves represents a stable working point of the cycle, dictated by the ejector performance in terms of entrainment ratio. When this occurs, the ejector can accurately control the detector outlet pressure and therefore temperature, being in two-phase state. However, two possible scenarios can occur during operation: the flow through the detector for any reason (i.e. load change) may need to be reduced (case 1) or to be increased (case 2). In both cases the ejector is the device used for conditioning the detector. In the first case, turning down the metering valve installed upstream of the suction nozzle (Figure 8) increases the pressure lift seen by the ejector inducing a reduction of the flow entrained. In Figure 9 the new intersection point is given by the same ejector curve and new detector curve which accounts for the extra ΔP introduced by the valve (red dotted line). An excessive closing of the valve leads to a fast increase of the vapor content due to the reduction of the flow invoked by the ejector under the same heating power. In the second case the flow needs to be increased and therefore starting point 2 can be seen as a deteriorated flow scenario. The entrainment potential of the ejector is enhanced by upgrading the ejector curve mainly varying the motive conditions, especially in terms of pressure. The performance map is adapted to load change conditions by varying the motive nozzle entering conditions. This in principle translates to a floating control of the discharge pressure while simultaneously controlling the receiver pressure via the CGBV to the desired setpoint.

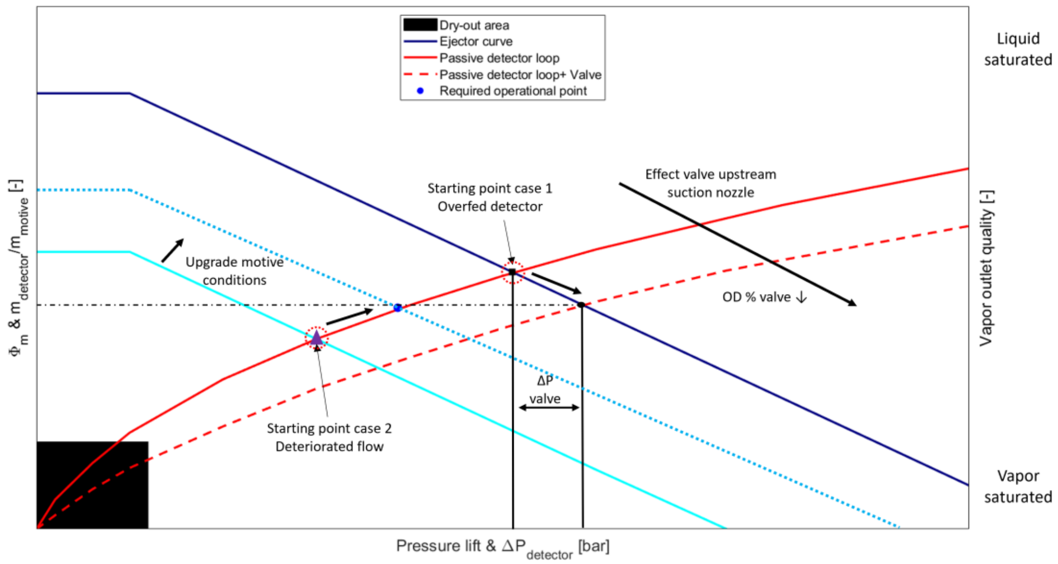

Figure 9: Ejector characteristic curve (light blue & blue) & normalized detector curve (red) respect to the motive flow for a fixed outlet temperature in the detector (-70 °C), considering the detector powered (450 W). The blue circle represents the desired operational point (flow) in the detector while the black square and purple triangle illustrate two different initial flow conditions through the detector which require an adjustment of the valve upstream of the suction nozzle or modulation of the ejector motive conditions (case 1 and 2, respectively).

7. Supercritical operation

The cycle presented above undergoes different scenarios during the detector's lifetime. Those working regimes cover both supercritical and transcritical operation, due to the combination of krypton properties and gradual cooldown of the detectors. The cycle start-up represents the first challenge (Figure 10): detectors are light-weight components with a non-uniform and limited heat capacity over all the structure. Therefore, to address a gradual cooldown, it is mandatory to control the fluid temperature entering the detectors. The first step is to fill the stagnant loop with an appropriate krypton mass inventory to reach the desired starting pressure (from point A to B). An improper charge can negatively affect the operation. It can lead to a mismatch in the initial pressure of the system compared to the established pressure startup procedure. If the pressure is excessively high additional mass is needed, while lower pressures pose a greater risk of fast cooling. The magnitude of the specific heat capacity which is described by the distance between the isothermal lines, under lower pressures, causes a larger temperature gradient per unit of mass. When the compressor is turned on the krypton fluid within the high-pressure leg becomes more dense displacing mass from the intermediate pressure side. A high volume ratio dampens this effect, though not entirely. In fact, the increase of the high pressure as a function of time is the main factor to consider. The rate at which the pressure increases can lead to possible thermal shock scenarios: the compressor discharge temperature would increase and the inherent delay of the high-temperature system (CO_2) in responding to an abrupt load change in the gas cooler may not satisfy process constraints, especially concerning the precise temperature control on the sensor. Any increase of the cycle pressure if not followed by a proper temperature control leads to density change, which in turns corresponds to a mass displacement and variation of the intermediate-low pressure levels. This action activates a sequence of transients that may bring the cycle out of the wanted operational envelope. Motivated by this, a dedicated control logic must be implemented. Heat rejection and high-pressure regulation are coupled to ensure a pressurization of the detector with as little flow as possible throughout all supercritical cooldown scenarios. Any injection or withdrawal of mass to/from the system can cause instabilities in terms of temperature fluctuations and longer time to achieve steady-state conditions. In this sense, volume ratios between the different sections of the cycle are important parameters to be predicted in order to provide the best control logic for the inventory control management. The latter refers to the common name used to describe the charge control of a CO_2 supercritical Brayton cycle [30], which is extended and used here. As a representative example, a simplified representation of the cycle on the p-h diagram is illustrated in Figure 10 where the non-active components have been excluded for sake of clarity.

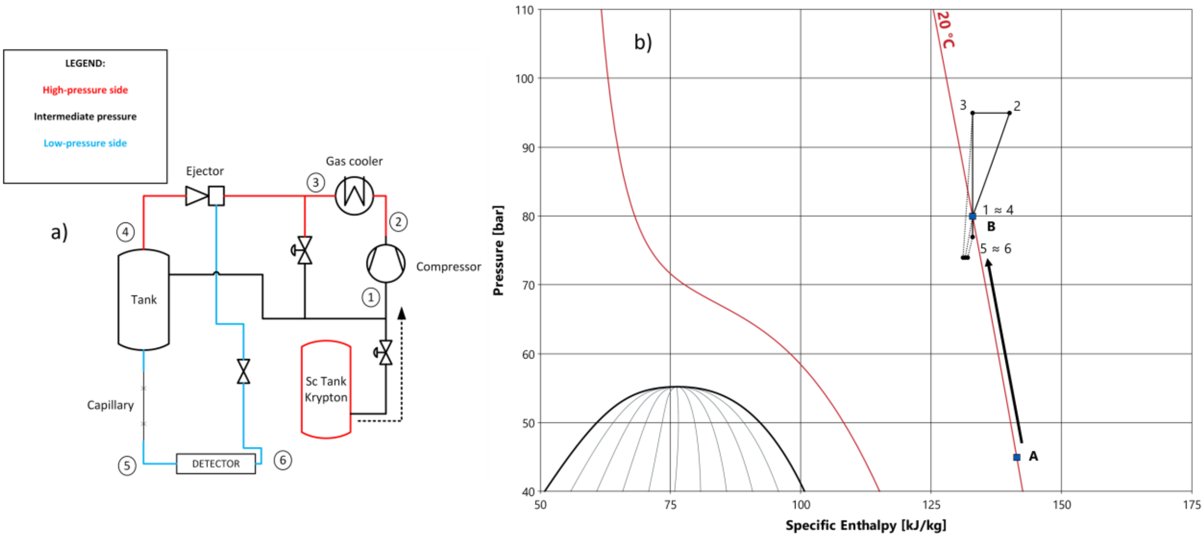

Figure 10: Simplified architecture of the krypton cycle during startup (a) and associated representation in the pressure-enthalpy diagram (b).

After stabilizing the cycle, the supercritical cooldown begins. The high-pressure side is cooled, bringing the cycle towards the colder area. The colder the temperature, the denser the fluid becomes. In the cycle only one pressure level can be actively controlled without any external loop (i.e. charging tank). Although one pressure level is controlled, the remaining two are affected by the remaining mass distributed as a function of their volume, pressure and temperature (density). Therefore, to sustain the cycle pressure, to avoid a fall into the two-phase area with consequent thermal shock, the high-pressure tank can inject mass into the system. Figure 11 (a) illustrates the extra charge required to sustain a pressure of 70 bar considering a volume of 1 liter. It is assumed that the pressure lift provided by the ejector is 1.5 bar between the tank and the detectors, which allows to maintain a small temperature gradient during the whole transition (see Figure 11 (b)). Therefore, maintaining a constant Δp along the loop (tank-suction nozzle ejector) protects the detector from fast overcooling once the tank pressure and temperature are well controlled. It is expected that the flow would increase, for the same pressure drop, while moving towards the colder area. This can be deducted by the supercritical fluid which behaves like a gas at warmer temperatures.

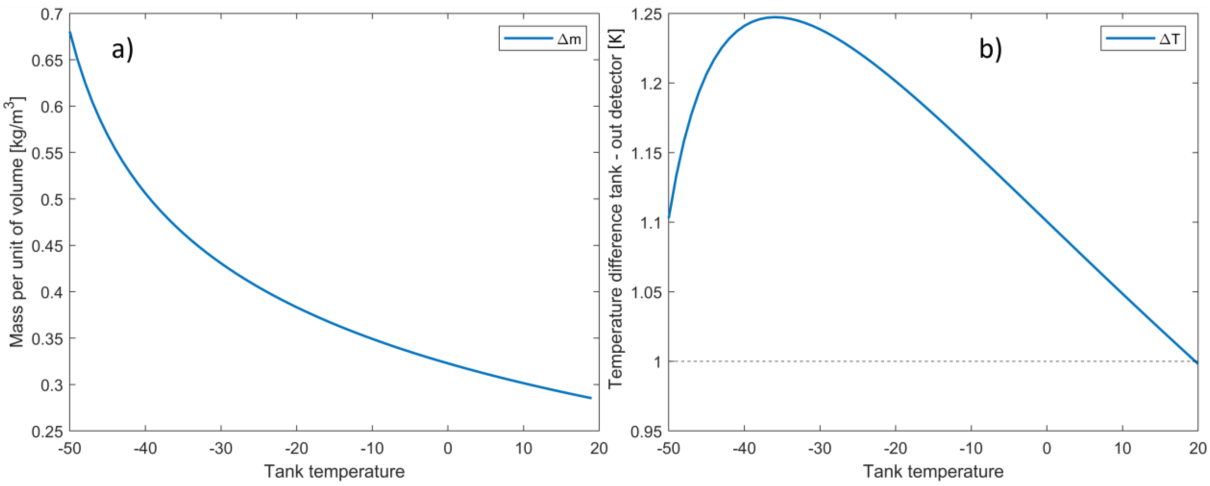

Figure 11: Charge upgrade during gradual cooldown of a system volume of 1 liter to maintain 70 bar pressure (a). Temperature difference between the tank (70 bar) and outlet of the detector while maintaining a fixed Δp of 1.5 bar (b).

During the duration of the supercritical cooldown with no power to be dissipated, only the first stage of gas cooling is active. It needs to reject the heat generated by the compressor only. Once the detector is powered, the second gas cooler is activated to reach thermal stability of the cycle.

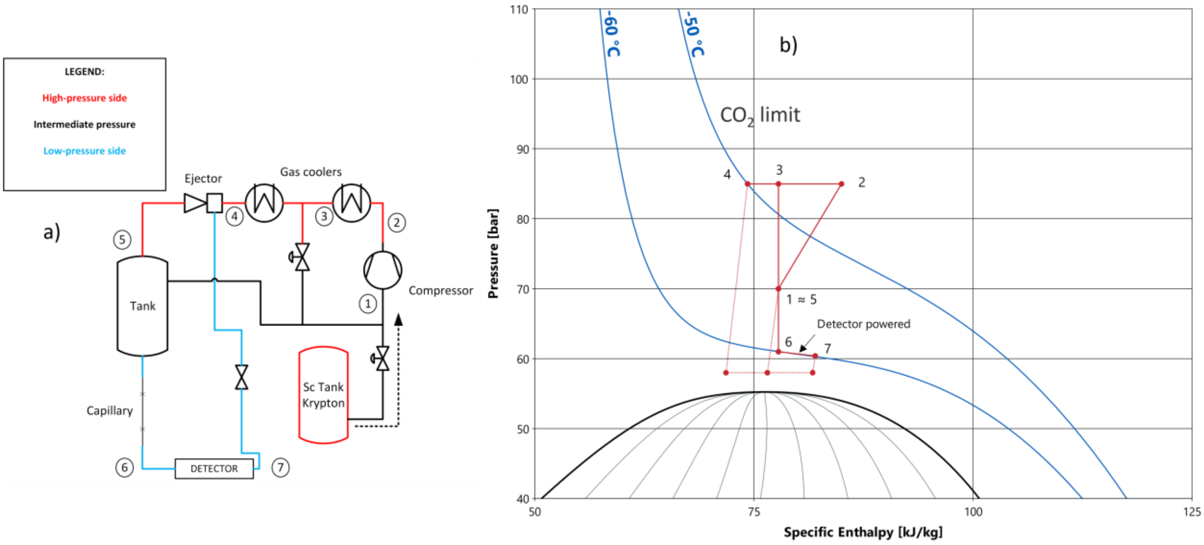

Figure 12: Simplified architecture of the krypton cycle during supercritical operation (a) and associated representation in the pressure-enthalpy diagram (b).

The thermodynamic limitation of the cycle is given by the triple point of CO_2: colder temperatures than -50/-55°C are not achievable due to the already low evaporating temperature of the high-temperature circuit. Furthermore, when the detector is powered (5-6) different legs of the cycle are characterized by different density zones. In the high-pressure side the fluid is denser, and it stores more mass compared to the preceding scenario where the detector was unpowered. The extra mass is displaced from the intermediate pressure side with a consequent depressurization of the intermediate-low pressure level, according to the mass movement towards the high-pressure side. Volume ratios between different sections of the cycle are extremely important to anticipate any action to be performed, either charging or discharging, they also have a drastic impact on the cycle dynamic. It is unpractical to continuously perform an injection or withdrawal of mass considering the extreme variability of the detector load profile. A larger volume on the intermediate-low pressure level can alleviate those oscillations but still a slight change of the operational point in the tank could occur. If this happens and assuming that the mass stored is insufficient to maintain the tank pressure at the desired setpoint, the valve upstream of the suction nozzle can be potentially used to reduce the entrained flow by the ejector maintaining almost unchanged the detector setpoint.

Detector cooling in the supercritical state resembles a gas heating process: pressure drops along the detector are welcome to promote an isothermal process while a larger flow potentially protects the detector from warming up. Indeed, if the flow through the detector decreases, the heat picked up by the krypton flow would correspond to a larger enthalpy change making the outlet the warmest spot, differently than in an evaporative process.

8. Transcritical cycle

If the detector needs colder temperatures, an evaporative cooling method is possible. The cycle must migrate from the supercritical to the transcritical area, gradually reaching new steady-state conditions. To perform this transition, charge shall be removed from the cycle causing a pressure drop in the system. When the supercritical tanks turn into a phase separator, the concept of the cycle aligns with that of a traditional ejector vapor compression system. Now the internal heat exchanger and the concentric lines are used to deliver superheated vapor (state point 6 -1) and subcooled fluid at the capillary inlets (state point 7-8), respectively. A partial bypass of the liquid is required before expanding through the capillary due to the compressibility of liquid krypton at high-pressures (state point 9). The CGBV (state point 3 – 1) still works as a capacity regulator, in the same manner as a variable speed drive compressor would. A parallel modulation of the latter together with the controllable ejector geometry ensures a precise control of the detector outlet temperature, as well as of the receiver pressure.

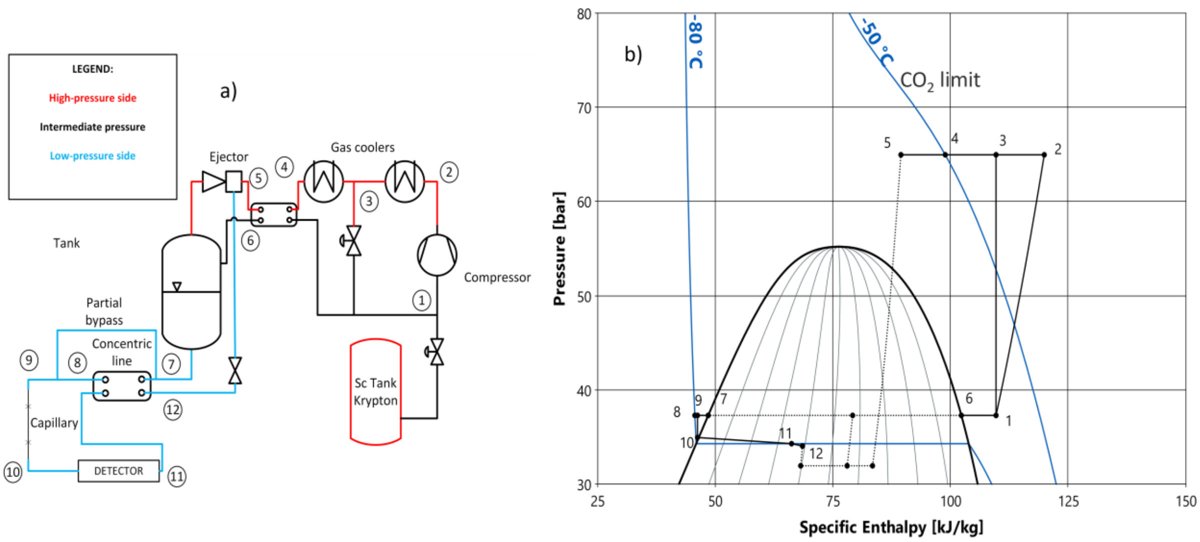

Figure 13: Simplified architecture of the krypton cycle during transcritical operation (a) and associated representation in the pressure-enthalpy diagram (b).

9. Technical challenges for the krypton demonstrator

The new cooling concept developed needs to be experimentally tested. In preparation for the experimental campaign, thermal design and consequent dynamic modelling of the full cycle is required and extremely helpful to understand the complex dynamics, as well as for improving the robustness of the necessary control logic to handle the different transient scenarios. The krypton prototype is currently under construction in Varmeteknisk laboratory at NTNU (Trondheim). However, many challenges arise from using the rare gas krypton that can be summarized as follows:

- Noble gases such as neon, krypton, xenon are extremely expensive compared to conventional fluids, for instance CO_2. They are harvested exclusively from air as byproduct in large air separation units via cryogenic distillation of air. Their main use covers window insulation and lighting (krypton), semiconductors (neon) and as detector material in investigation of dark matter (xenon) whilst their use as refrigerants has not been explored so far.
- The cost of krypton is less than Xenon due to higher abundance in the air (≈ factor 10) but they both suffer of high-price variations according to the market dynamic and continuous technological improvements (i.e. LEDs applications do not longer required krypton). The estimated price in [31] could not anticipate the recent world events and the market is not transparent. Two major rare gas suppliers were Russia and Ukraine but after Russia's invasion the supply market was strongly affected, remaining so until alternative producers emerge. Although Russia is still producing those gases, international sanctions will isolate them from the global market. Potential alternatives are China and US, while Germany remains the only reliable supplier in Europe. To understand the magnitude of change for krypton, its price quadrupled in the first months of 2022 in Japan [32].
- The cost of krypton and operation in the supercritical state require reduction of the system volume to limit the refrigerant charge needed to operate at high pressures.
- As krypton has never been used before in a vapor compression system, specific Krypton-based components are not available in the market. Therefore, high-pressure CO_2 rated components such as compressor and gas coolers will be used in the prototype. This constraint affects the ideal system design which would require the supercritical tank to be the largest volume in the system. By doing so, rapid changes of temperature and pressure can be alleviated by damping the gradients through a larger volume, considering that the tank represents the "entering conditions" to the detector. Even by using a very small CO_2 compressor for extremely low capacity, the compressor volume could store the largest amount of mass of the system, strongly impacting the behavior of the cycle. This is normally the opposite in a two-phase system, where the compressor is operated in the low-density vapor region and large part of the mass is stored in the buffer tank and condenser (due to the liquid phase).

10. Theoretical assessment of typical operational point of the krypton cycle

As illustrative examples, numerical simulations of the supercritical and transcritical cycle have been performed to analyze the thermal behavior of the cycle under different operating conditions. The cycle layout was implemented within the simulation environment Dymola using the TIL-Suite and TILMedia-Suite, which are a commercial Modelica model library for thermal components-systems ([33,34]) and a software package for determination of the thermophysical properties [35], respectively. The assumptions used for the modelling are summarized in Table 1. Considering the multi cooling branch layout around the detectors, three cooling branches were selected and used in the examples. Details of heat transfer and pressure drop correlations, as well as geometrical characterization of the components are not reported because it is out of the scope of this work.

Table 1: Assumptions used in thermal modelling of the cycle.

Component	Assumption
Compressor	Fixed isentropic and volumetric efficiency (60%)
Ejector	Constant efficiency (25%)
Detector	Load varied in the range 0-150 W
Detector cooling pipe (standard as in use with CO_2)	Length = 1 [m], inner diameter 2 [mm]

The first two simulations investigate supercritical operation. The system was initially simulated without heat dissipation from the detector, resembling one of the points encountered during the supercritical cooldown. As described in Figure 10, only the first gas cooler is active to dissipate the thermal load introduced by the compression. The ejector works as a flow circulator through the detector while guaranteeing a minimal change in temperature and pressure along the loop. Figure 14 shows the thermodynamic points of the cycle in the pressure-enthalpy diagram.

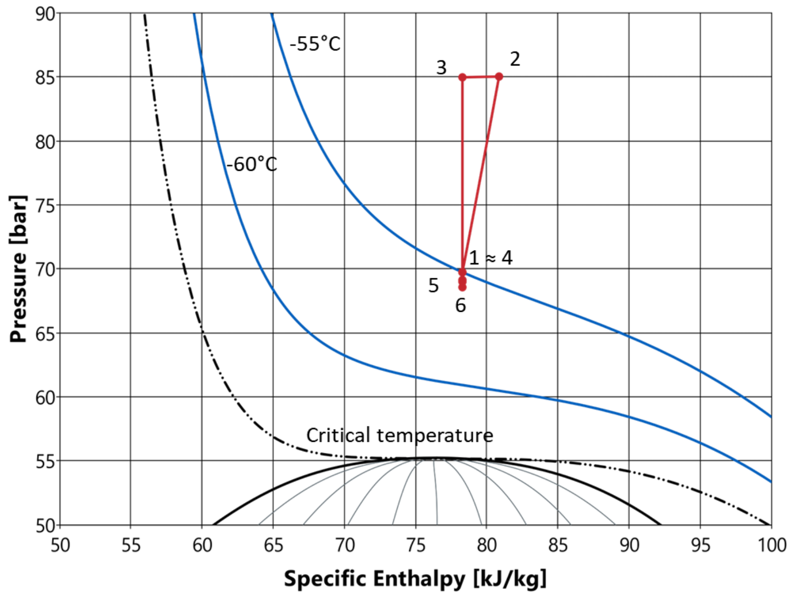

Figure 14: Steady-state result during supercritical operation with detector unpowered. Schematic of the cycle in the p-h diagram (points corresponds to Figure 10).

Secondly, when the detector is powered the second gas cooler is switched on to dissipate the thermal power absorbed (Figure 15). The operational point in the detector has been selected considering one of the pseudocritical points illustrated in Figure 2, which can be interpreted as performance map to achieve the best thermal performance offered by the fluid in supercritical state. As described earlier, gas heating in the supercritical state (points 5-6) may cause a temperature increase between the inlet and the outlet, according to the pressure gradient along the detector which helps to follow an almost isothermal process.

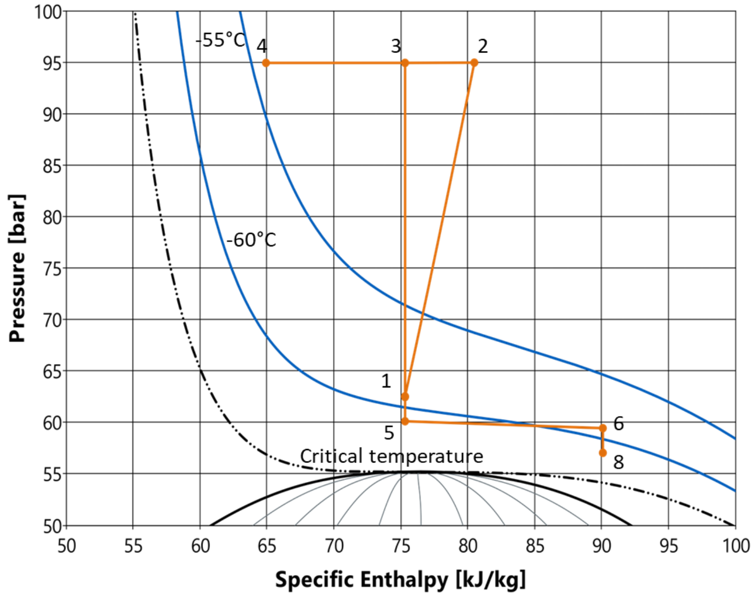

Figure 15: Steady-state result during supercritical operation with detector powered. Schematic of the cycle in the p-h diagram (points referred to Figure 12) considering a setpoint around -60°C. Additional pressure drops defined by the points (6-8) correspond to the return line (tube-in-tube) which is bypassed on the inlet side, due to the single phase state of the fluid.

In the case simulated, the entrainment potential of the ejector is increased by further raising the high pressure to cope with the power absorbed by the detector. An overflow through the detector would lead to colder fluid temperatures, as well as having an impact on the mass distribution within the system. The detector setpoint was chosen to ensure cooling while exploiting the region with high values of specific heat capacity (Figure 16). However, a degradation of the specific heat capacity is observed by moving further from the inlet. The reason of such degradation is explained at the end of this chapter. Low viscosities in the supercritical state are observed: in the region of interest (above the critical point) the fluid presents viscosity levels like the gas phase while having high densities typical of the liquid phase.

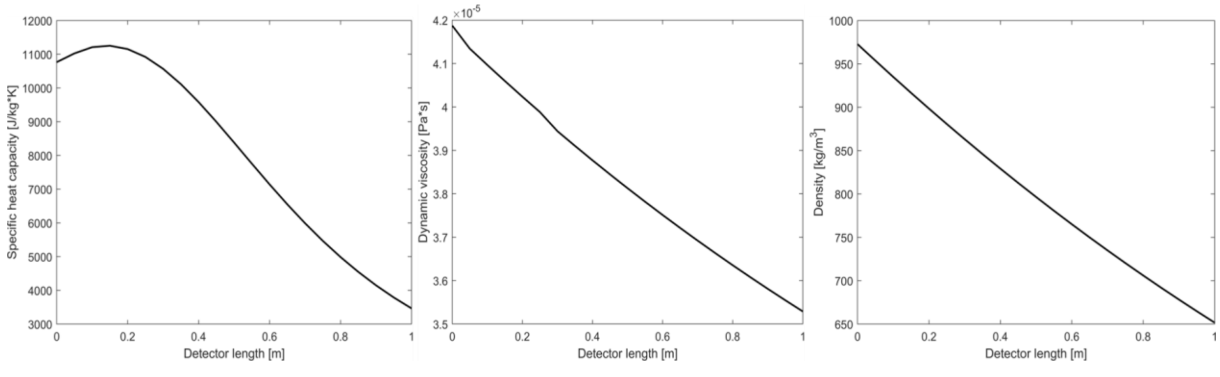

Figure 16: Variation of the specific heat capacity, viscosity and density along the detector during gas heating.

At last, the krypton cycle was simulated for the coldest working conditions in the detector (-70°C). This scenario refers to the transcritical operation (Figure 17). The main difference compared to a conventional ejector cycle is the great amount of liquid in the exhaust two-phase flow at the detector outlet. Thermodynamic limitations are given by the CO_2 triple point which limits the lowest heat rejection temperature achievable in the second gas cooler. The ejector motive conditions are, for the reason above, limited to “warmer” temperatures but with the flexibility of adjusting the pressure by moving the needle installed in front of the motive nozzle throat in and out.

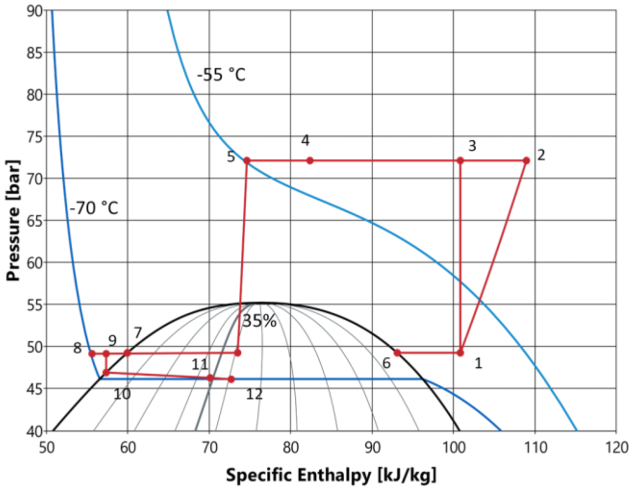

Figure 17: Steady-state result during transcritical operation with detector powered with setpoint set to -70°C (outlet vapor quality ≈ 35% as required by design). Schematic of the cycle in the p-h diagram (points corresponding to Figure 10).

The difference between supercritical to transcritical operation can be seen in the pressure-temperature distribution along the detector, as shown in Figure 18. During gradual cooldown of the detectors (left side), the flow entrained by the ejector is relatively small as cooling is not yet required. Without power absorbed, the temperature changes by approximately 0.1 K. During gas heating conditions (supercritical state), the pressure decreases along the pipe length while the temperature increases by approximately 1.6 K. The detector cooling channel may potentially be designed to introduce larger pressure drops to follow up the isothermal line throughout the gas heating process. Typically, a temperature difference of 5 K is allowed between the inlet and the outlet. Considering the flow boiling conditions occurring at colder temperatures, the performance in supercritical and transcritical states can be traded off against each other. The pressure does not decrease in a linear manner as typical for the single-phase state: in supercritical state above the critical point sharp changes of density and viscosity occur. Overall (in-out) it resembles a two-phase flow behavior near the critical point. It is worth noticing that in the right plot (flow boiling) the pressure profile lies between a linear and a parabolic curve. The two-phase correlation used [36] in the evaporator was characterized by a relatively low (below 2) two-phase multiplier. The Friedel correlation is based on the separated flow approach wherein the estimation of the two-phase pressure drop involves treating the entire flow as single-phase liquid while accounting for the larger pressure drops given by the vapor phase through the two-phase multiplier. High reduced pressure and low vapor quality as required by detector cooling are the main causes of such behavior. Closer to the critical point vapor and liquid density tend to be the same: the slip ratio and vapor velocity decreases, resembling a homogeneous vapor-droplet flow. More importantly, in a more homogenous flow the dependency of pressure drops on the vapor content is weaker. This improves the equalization of flows in different cooling branches with different heat loads at high reduced pressures.

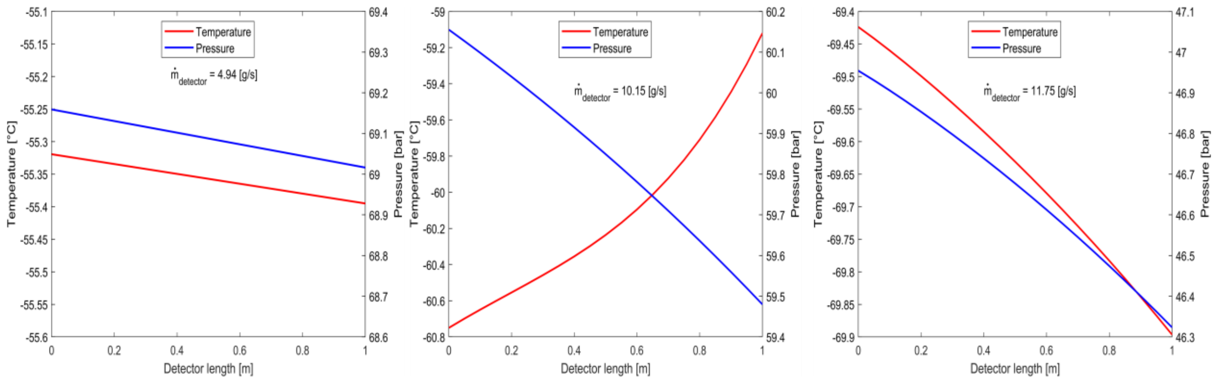

Figure 18: Temperature-pressure distribution in the detector for three different cases: supercritical operation with detector unpowered and powered (left and middle), flow boiling operation during transcritical operation (right side).

In section 3, a fluid case study was carried out to identify the optimal tube diameter. The comparison was made with respect to the two-phase area: as one specific tube diameter does not lead to the best thermal performance over a wide range of reduced pressure, neither does it in supercritical state. If then, the detectors need temperatures in the range of -60 down to -80°C, three possible scenarios exist. The cooling channel inside the detectors can be optimized based exclusively on the supercritical state, on the two-phase area or considering a trade-off between the two cases. Pressure drops which are normally unwanted during vaporization of the fluid promote a more homogenous fluid temperature profile along the detector during gas heating near the critical point. Nevertheless, for a given geometry, the rise of the fluid temperature can be reduced by overflowing the detector, corresponding to a smaller enthalpy change. This in turn has an effect at system level: overflowing the detector means an increase of the total pressure lift provided by the ejector due to the fixed fluid resistance introduced by the capillary upstream of the detector. As a side-effect, the whole cycle moves up in pressure requiring extra krypton mass for the pressurization. The desired operational strategy, which is also affected by temperature requirements from the detectors, is therefore object of further study.

An illustrative example of a fluid case study in supercritical state focusing exclusively on pressure drops is presented below in Figure 19. The input conditions (p-T) and the heat load (150 W, equally distributed[2]) were fixed, while the channel diameter and the flow rate were varied. The flow rate can be adjusted by the ejector up to a certain extent, dependent on its design. The range of channel size interesting for detector cooling is around or below 2 mm, which was previously considered as optimal for flow boiling operation. In that area a colder outlet temperature than the inlet. Although the estimation of the pressure drops is based on a single-phase correlation not developed for supercritical fluids, the optimization concept does not change. An increase or decrease of the mass flow rate influences the outlet fluid enthalpy. A smaller pipe diameter, for a given mass flow rate, produces larger frictional losses along the cooling pipe. The combination of these effects can be seen in the optimization study in Figure 19. A more intuitive representation can be found in Figure 19 (b-c), where pressure-temperature profiles are plotted in the pressure-enthalpy diagram. The fluid temperature can increase, decrease or have a sinusoidal profile. A similarity can be considered between gas heating and the vaporization process: excessive low flow rates have a potentially harmful effect on the integrity of

[2] It is common to consider for sake of simplicity constant heat flux conditions along the detector stave. The heat load dissipated is a function of the sensor's temperature, which in turn is dependent on the temperature gradient (in first approximation only dependent on the fluid heat transfer coefficient if thermal resistivity of the support structure is considered temperature-independent). However, a short gap between the different sensors glued to the detector stave is typically present, resulting in alternating powered and unpowered sections.

the sensors in both cases. Indeed, during flow boiling low flow rates can cause dry-out with a reduction of the heat removal capability, mainly due to the low thermal conductivity of the vapor phase. During gas heating, regardless of the local fluid heat transfer coefficient, the non-uniformity of the fluid temperature is in principle reflected in the temperature gradient along the thermal path between the sensor and the cooling pipe. Furthermore, larger enthalpy changes suggest moving away from the region near the pseudocritical points with an expected degradation of the heat transfer performance (drop of the specific heat capacity). Figure 2 showed that the peaks in the specific heat capacity quickly decreased with increasing temperature. Introducing pressure losses does not only help to trigger a more uniform flow temperature distribution along the detector but also to remain close to the critical point. The area characterized by those peaks is also very narrow and temperature dependent. This suggests to design for a limited enthalpy gain of the fluid, while achieving a nearly zero or negative temperature gradient between the inlet and the outlet.

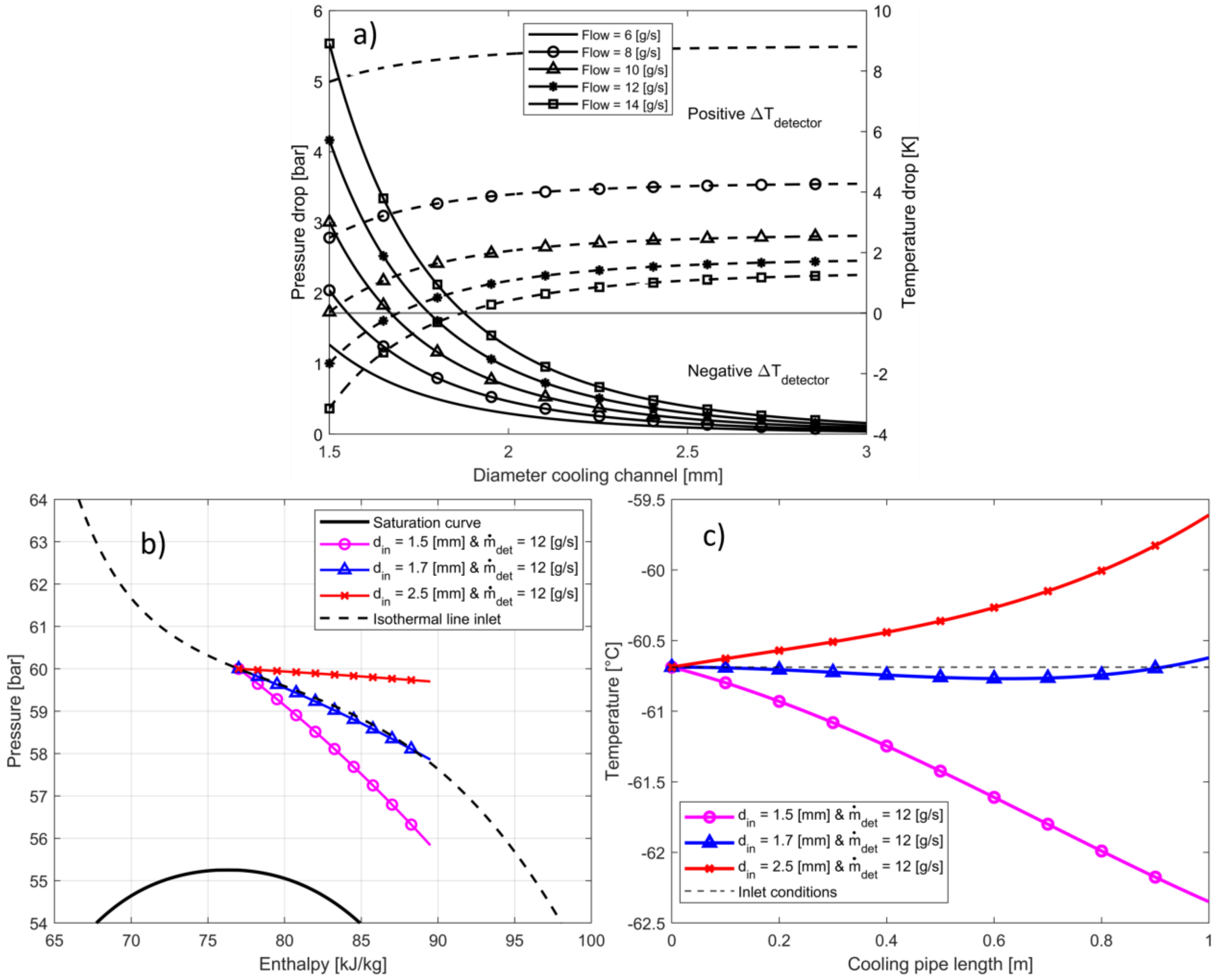

Figure 19: Fluid-study optimization (a) of the cooling channel during supercritical operation (solid line = ΔP, dotted line = ΔT, d_{in} = inner diameter). Entering conditions are fixed (p = 60 [bar], h = 77 [kJ/kg]). The Swamee-Jaime correlation was used for the pressure drop calculation [37]. Pressure profile along the detector for a given flow of 12 [g/s] while changing the channel diameter (b). Temperature distribution (c) along the pipe for the cases plotted in (b).

11. Conclusion

Based on the HL-LHC plan, a future upgrade of the detector is planned to take place in 2034. To address the challenges arising from a highly irradiated environment, a cooling fluid allowing for colder operation than with CO_2 is required. A fluid-based comparison showed that the noble gas krypton is a promising candidate for the thermal management of the detectors. The gradual cooldown occurs in supercritical phase thus requiring a new cooling technology with a dedicated control logic. A new ejector-supported cycle is presented with a short description of the transient scenarios occurring during the detector lifetime. Some design guidelines have been drawn based on analysis of the fluid behavior in the supercritical and two-phase state, emphasizing the need of a distinct or combined optimization of the cooling channel inside the detector. The new krypton cycle is a candidate for the Vertex Locator (Velo) of the LHCb detector and for the NA62 experiment, which are experiments at CERN of limited cooling capacity (in the order of few kW).

Acknowledgements

This research work is supported by the European Union's Horizon 2020 research and innovation program, 'AIDAInnova project' (grant number 101004761).

References

[1] G. Beck, G. Viehhauser, Analytic model of thermal runaway in silicon detectors, Nuclear Instruments and Methods in Physics Research Section A: Accelerators, Spectrometers, Detectors and Associated Equipment 618 (2010) 131–138. https://doi.org/10.1016/j.nima.2010.02.264.

[2] ATLAS collaboration, ATLAS Inner Detector: Technical Design Report - Vol I, CERN, 1997.

[3] D. Attree, The evaporative cooling system for the ATLAS inner detector, J. Inst. 3 (2008) P07003. https://doi.org/10.1088/1748-0221/3/07/P07003.

[4] M. Battistin, The Thermosiphon Cooling System of the ATLAS Experiment at the CERN Large Hadron Collider, International Journal of Chemical Reactor Engineering 13 (2015) 511–521. https://doi.org/10.1515/ijcre-2015-0022.

[5] B. Verlaat, M. Van Beuzekom, A. Van Lysebetten, CO2 cooling for HEP experiments, Topical Workshop on Electronics for Particle Physics (2008) 328–336. https://doi.org/10.5170/CERN-2008-008.328.

[6] B. Verlaat, Controlling a 2-phase CO2 loop using a 2-phase accumulator, 22nd IIR International Congress of Refrigeration (2007).

[7] B. Verlaat, A. Lysebetten, M. van Beuzekom, CO2 cooling for the LHCb-VELO experiment at CERN, in: Proceedings on the 8th IIF/IIR Gustav Lorentzen Conference on Natural Working Fluids, Copenaghen, 2008.

[8] P. Tropea, J. Daguin, A. D'Auria, J. Godlewski, M. Ostrega, S. Pavis, P. Petagna, H. Postema, L. Zwalinski, J. Noite, B. Verlaat, Design, construction and commissioning of a 15 kW CO2 evaporative cooling system for particle physics detectors: lessons learnt and perspectives for further development, in: Proceedings of Technology and Instrumentation in Particle Physics 2014 — PoS(TIPP2014), SISSA Medialab, 2015: p. 223. https://doi.org/10.22323/1.213.0223.

[9] B. Verlaat, M. Ostrega, L. Zwalinski, C. Bortolin, S. Vogt, J. Godlewski, O. Crespo-Lopez, M.V. Overbeek, T. Blaszcyk, The ATLAS IBL CO2 cooling system, Journal of Instrumentation 12 (2017) C02064. https://doi.org/10.1088/1748-0221/12/02/C02064.

[10] R. and A.-C.E. American Society of Heating Inc, 2018 ASHRAE® Handbook: Refrigeration, American Society of Heating, Refrigerating and Air-Conditioning Engineers, 2018.

[11] B. Verlaat, P. Petagna, R&D for a colder future in HEP, in: Forum on Tracking Detector Mechanics, 2019.

[12] ECFA Detector R&D Roadmap Process Group, The 2021 ECFA detector research and development roadmap, (2020). https://doi.org/10.17181/CERN.XDPL.W2EX.

[13] P. Petagna, B. Verlaat, A. Francescon, Two-Phase Thermal Management of Silicon Detectors for High Energy Physics, in: Encyclopedia of Two-Phase Heat Transfer and Flow III, World Scientific, 2018: pp. 335–412.

[14] G.D. Nicola, G. Giuliani, F. Polonara, Blends of CO2 and N2O as working fluids in cascade cycles, in: IIR International Conferences, 2005.
[15] M. Kauffeld, T. Maurath, J. Germanus, E. Askar, N2O/CO2-Mixtures as Refrigerants for Temperatures below-50° C, International Journal of Refrigeration 117 (2020) 316–327.
[16] J. Furtado, F. De Proft, P. Geerlings, The Noble Gases: How Their Electronegativity and Hardness Determines Their Chemistry, J. Phys. Chem. A 119 (2015) 1339–1346. https://doi.org/10.1021/jp5098876.
[17] X. Lei, R. Peng, Z. Guo, H. Li, K. Ali, X. Zhou, Experimental comparison of the heat transfer of carbon dioxide under subcritical and supercritical pressures, International Journal of Heat and Mass Transfer 152 (2020) 119562. https://doi.org/10.1016/j.ijheatmasstransfer.2020.119562.
[18] A.D. Hellenschmidt, Experimental studies on small diameter carbon dioxide evaporators for optimal Silicon Pixel Detector cooling, PhD Thesis, U. Bonn, 2020.
[19] M. Gupta, Calculation of radiation length in materials, CERN, Geneva, 2010. https://cds.cern.ch/record/1279627.
[20] The MathWorks Inc. (2022), MATLAB version: 9.12.0 (R2022a), (Natick, Massachusetts: The MathWorks Inc). https://www.mathworks.com.
[21] S.G. Kandlikar, A General Correlation for Saturated Two-Phase Flow Boiling Heat Transfer Inside Horizontal and Vertical Tubes, Journal of Heat Transfer 112 (1990) 219–228. https://doi.org/10.1115/1.2910348.
[22] L. Friedel, Improved friction pressure drop correlations for horizontal and vertical two-phase pipe flow, in: European Two-Phase Group Meeting, Ispra, Italy, 1979.
[23] P. Barroca, Modelling CO_2 cooling of the ATLAS ITk Pixel Detector, PhD Thesis, U. Grenoble Alpes, 2019. https://cds.cern.ch/record/2703341 (accessed October 16, 2023).
[24] P. Tropea, J. Daguin, P. Petagna, H. Postema, B. Verlaat, L. Zwalinski, CO2 evaporative cooling: The future for tracking detector thermal management, Nuclear Instruments and Methods in Physics Research Section A: Accelerators, Spectrometers, Detectors and Associated Equipment 824 (2016) 473–475. https://doi.org/10.1016/j.nima.2015.08.052.
[25] A. Cavallini, C. Zilio, Carbon dioxide as a natural refrigerant, International Journal of Low-Carbon Technologies 2 (2007) 225–249. https://doi.org/10.1093/ijlct/2.3.225.
[26] M.-H. Kim, J. Pettersen, C.W. Bullard, Fundamental process and system design issues in CO2 vapor compression systems, Progress in Energy and Combustion Science 30 (2004) 119–174. https://doi.org/10.1016/j.pecs.2003.09.002.
[27] S. Elbel, Historical and present developments of ejector refrigeration systems with emphasis on transcritical carbon dioxide air-conditioning applications, International Journal of Refrigeration 34 (2011) 1545–1561. https://doi.org/10.1016/j.ijrefrig.2010.11.011.
[28] S. Elbel, P. Hrnjak, Experimental validation of a prototype ejector designed to reduce throttling losses encountered in transcritical R744 system operation, International Journal of Refrigeration 31 (2008) 411–422. https://doi.org/10.1016/j.ijrefrig.2007.07.013.
[29] S. Elbel, N. Lawrence, Review of recent developments in advanced ejector technology, International Journal of Refrigeration 62 (2016) 1–18. https://doi.org/10.1016/j.ijrefrig.2015.10.031.
[30] A. Moisseytsev, K.P. Kulesza, J.J. Sienicki, Control system options and strategies for supercritical CO2 cycles., Argonne National Lab. (ANL), Argonne, IL (United States), 2009. https://doi.org/10.2172/958037.
[31] H. Elsner, Edelgase – Versorgung wirklich kritisch?, DERA Rohstoffinformationen, Berlin, 2018.
[32] K. Georgitzikis, E. D'elia, Rare Gases (Krypton, Neon, Xenon): Impact assessment for supply security, European Commission, 2022.
[33] W. Tegethoff, C. Schulze, M. Gräber, M. Huhn, N. Stulgies, C. Kaiser, M. Loeffler, TEMO: Thermische echtzeitfähige Modelle, Braunschweig, Germany (2011).
[34] C.C. Richter, Proposal of new object-oriented equation-based model libraries for thermodynamic systems, Braunschweig, Techn. Univ., Diss., 2008, 2008.

[35] C.W. Schulze, A Contribution to numerically efficient modelling of thermodynamic systems, dissertation, Technical University Braunschweig, Braunschweig Germany (2013).
[36] L. Friedel, Improved Friction Pressure Drop Correlation for Horizontal and Vertical Two-Phase Pipe Flow, in: 1979.
[37] P.K. Swamee, A.K. Jain, Explicit Equations for Pipe-Flow Problems, Journal of the Hydraulics Division 102 (1976) 657–664. https://doi.org/10.1061/JYCEAJ.0004542.

Nomenclature

Abbreviations and variable names

d	Diameter (mm)
Δp	Pressure drop (bar)
ΔT	Temperature drop (K)
OD	Opening degree (-)
IHX	Internal heat exchanger
$\dot{m}$	Mass flow rate (kg/s)
P	Pressure (bar)
Q	Heat load (W)
VHTC	Volumetric heat transfer coefficient (W/m^{3}K)
NBP	Normal Boiling Point (°C)
Greek symbols	
Θ_m	Mass entrainment ratio (-)
Subscripts	
det	Detector
in	Inner